

Supplementary Material

Supplemental Figure S1. Comparison of clonogenic survival fractions of various cancer cell lines after treatment with SAR302503 and Ruxolitinib.

Supplemental Figure S2. KRAS mutation by treatment sensitivities in NSCLC cell lines.

Supplementary Figure S3. Response of NCIH1944 xenografts to ionizing radiation.

Supplemental Figure S4. Top-ranked pathways in SAR sensitive NSCLC cell lines.

Supplemental Figure S5. Cancer growth and proliferation gene network in SAR-sensitive NSCLC.

Supplemental Figure S6. ROC analysis of SAR sensitivity by TSP-IRDS scores.

Supplemental Figure S7. Distribution of TSP-IRDS scores in clinical NSCLCs.

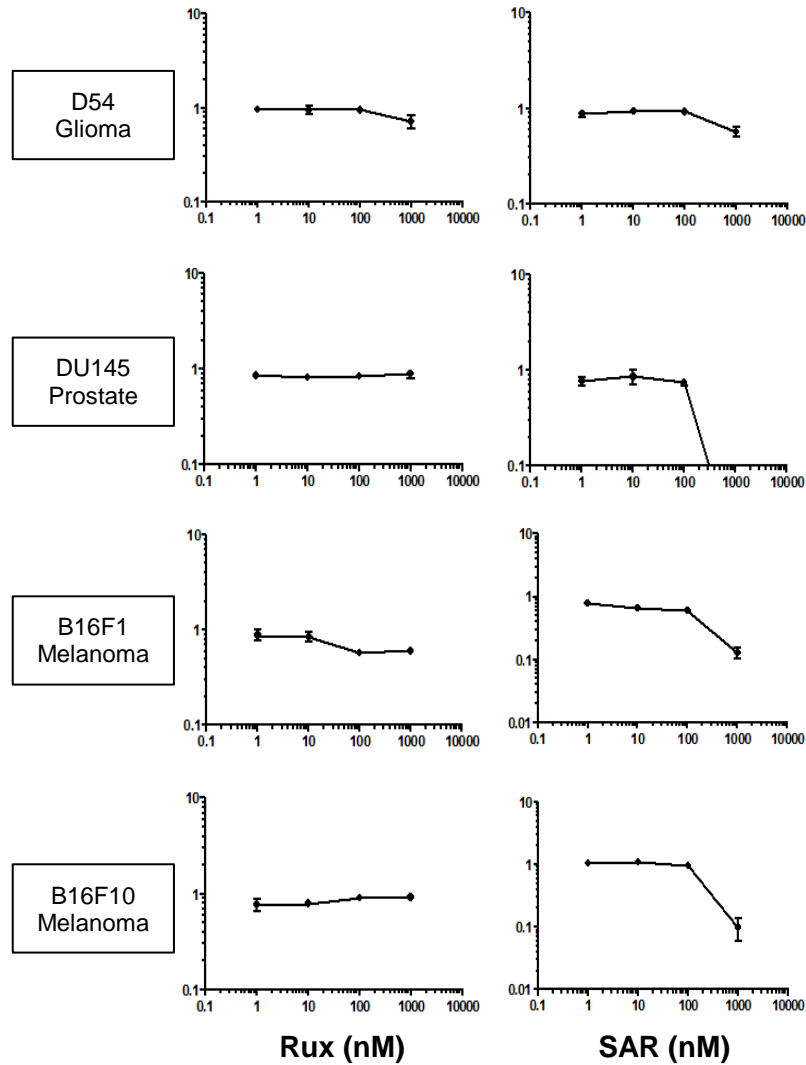
Supplemental Figure S8. TSP-IRDS predicts survival in clinical NSCLC.

Supplemental Figure S9. TSP-IRDS scores predict benefit of adjuvant cisplatin-based chemotherapy in clinical NSCLC.

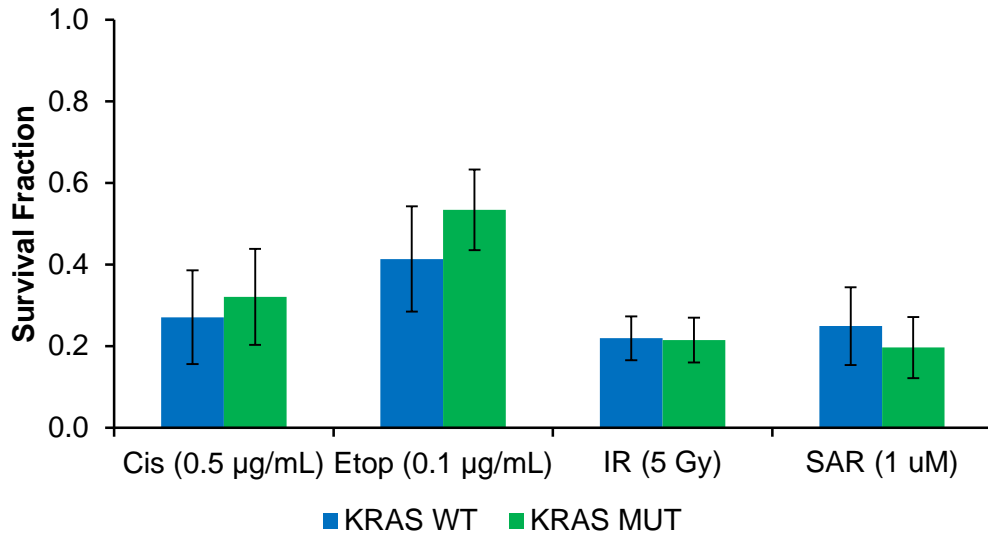
Supplemental Table S1. Clonogenic survival of NSCLC cell lines after cytotoxic therapy.

Supplemental Table S2. Gene expression patterns correlating with SAR sensitivity.

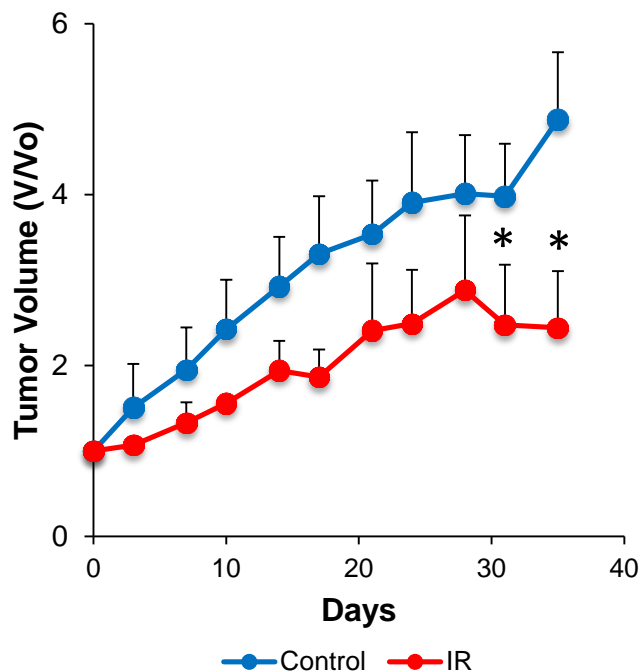
Survival Fraction



Supplemental Figure S1. Comparison of clonogenic survival fractions of various cancer cell lines after treatment with SAR302503 (SAR) and Ruxolitinib (Rux). Cell lines were plated in triplicate at densities ranging from 2×10^2 to 2×10^3 per 100 mm culture dish. Twenty-four hours after plating, the cell lines were treated with SAR or Rux at the above doses. Each cell culture plate was washed with 0.85% NaCl solution and stained with 2% crystal violet (Fisher Scientific). Colonies comprised of at least 50 cells were then manually counted at two weeks following treatment.

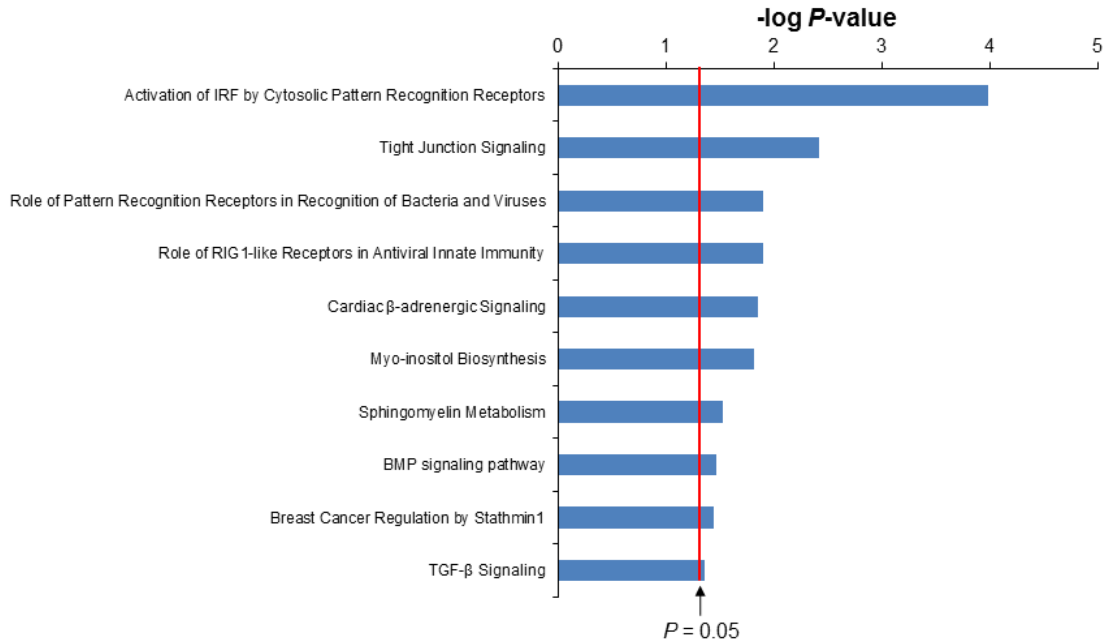


Supplemental Figure S2. KRAS mutation by treatment sensitivities in NSCLC cell lines. Survival fraction after treatment with cisplatin (Cis), etoposide (Etop), ionizing radiation (IR) and SAR302503 (SAR) were determined for 15 cell lines with corresponding KRAS mutation data (see Supplemental Table S1). Data represent mean values. Error bars represent S.E.M. Student's t-test demonstrated no significant differences in mean survival fraction in the comparisons of KRAS wild-type and KRAS mutant cell lines.



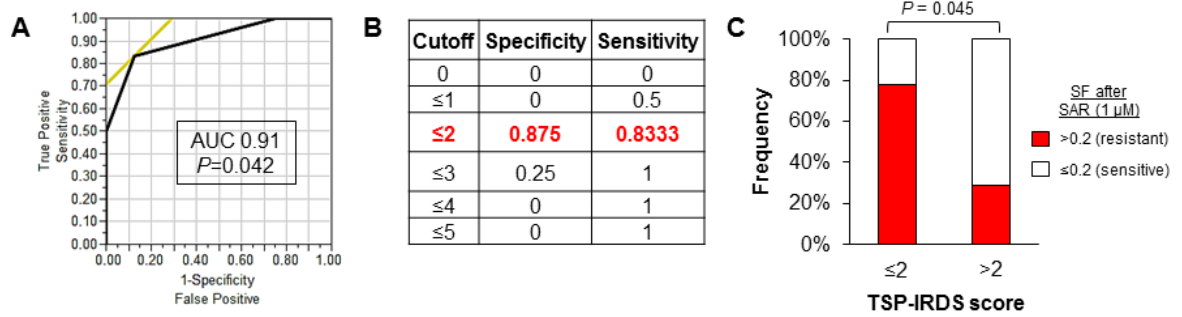
Supplementary Figure S3. Response of NCIH1944 xenografts to ionizing radiation.

In vivo growth of NCIH1944 tumor xenografts in athymic nude mice treated with ionizing radiation (10 Gy x 2) on days 2 and 3 after tumors reached an average volume of 150 mm³ as compared to control treated tumors. n=5 mice per group. Tumor volume, V. Initial tumor volume, V₀. P-values determined using Student's t-test. *denotes P-value ≤ 0.05.



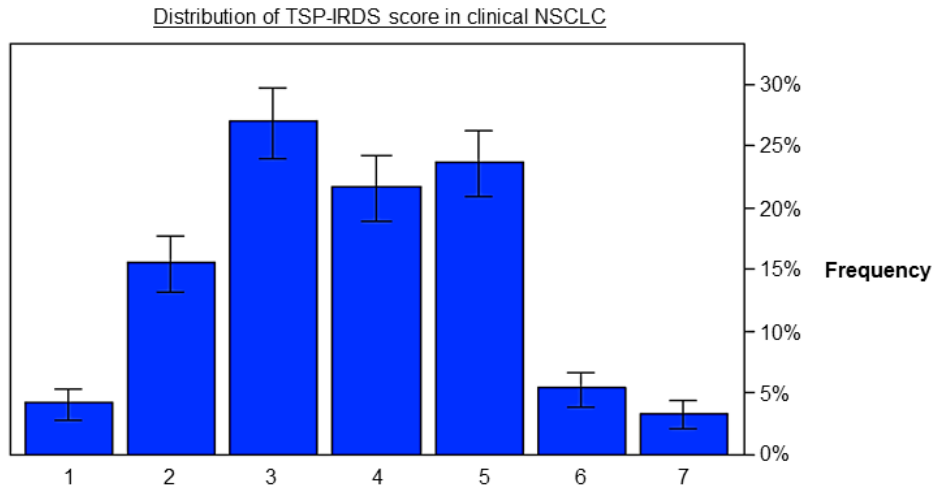
Supplemental Figure S4. Top-ranked pathways in SAR sensitive NSCLC cell lines.

Genes overexpressed in SAR-sensitive as compared to SAR-resistant NSCLC cell lines were analyzed using Ingenuity Pathway Analysis (IPA). Shown are top-ranked statistically significant canonical pathways over-represented in SAR-sensitive cell lines.

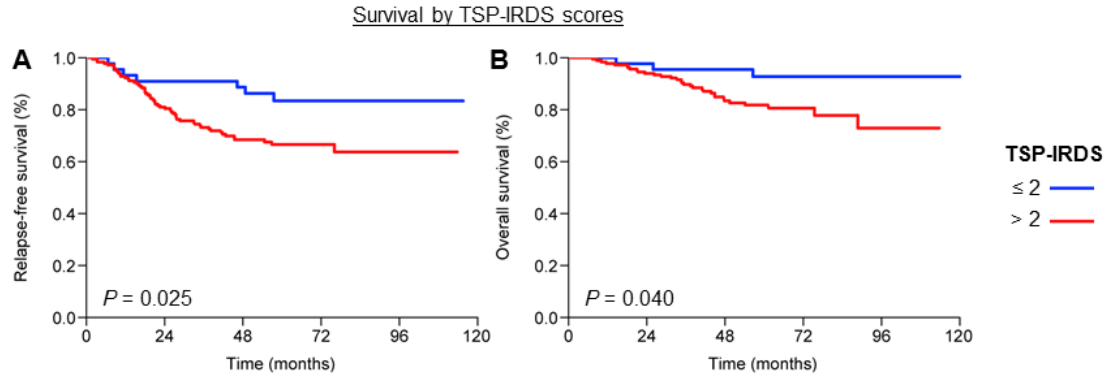


Supplemental Figure S6. ROC analysis of SAR sensitivity by TSP-IRDS scores. (A)

Receiver operating characteristic (ROC) curve analysis of SAR sensitivity as a function of TSP-IRDS score. Area under curve (AUC) = 0.91 ($P=0.042$). **(B)** TSP-IRDS cutoff of ≤ 2 provides a sensitivity of 0.83 and specificity of 0.88 in discriminating SAR resistant (low scores) and SAR sensitive (high scores) NSCLC cell lines. **(C)** Proportion of SAR-sensitive cell lines by TSP-IRDS score. P -value determined using Chi-square test.

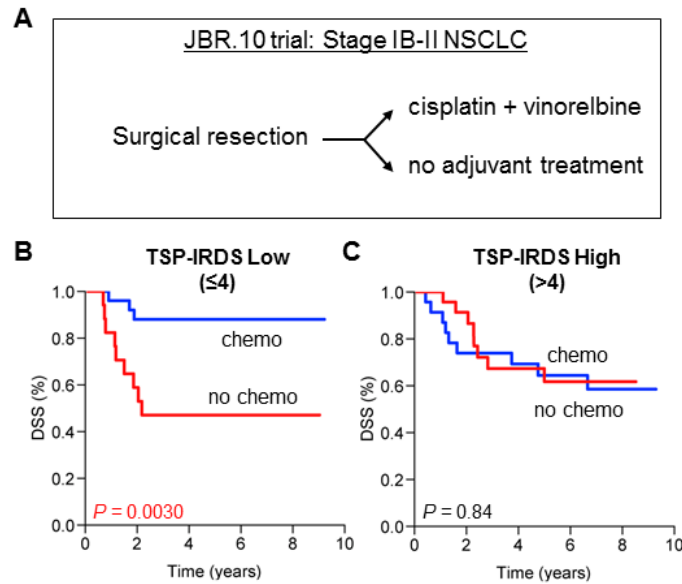


Supplemental Figure S7. Distribution of TSP-IRDS scores in clinical NSCLCs. TSP-IRDS scores were calculated using gene expression data from the GSE31210 dataset of 246 human NSCLCs. Data represent the frequency \pm standard error.



Supplemental Figure S8. TSP-IRDS predicts survival in clinical NSCLC. TSP-IRDS

scores were calculated using gene expression data from the GSE31210 dataset of 246 human NSCLCs. Patients were split into TSP-IRDS low (≤ 2 , n=48) and high (>2 , n=198) groups and assessed for relapse-free (**A**) and overall (**B**) survival using Kaplan-Meier analyses. *P*-values were determined using log-rank tests.



Supplemental Figure S9. TSP-IRDS scores predict benefit of adjuvant cisplatin-based chemotherapy in clinical NSCLC. (A) TSP-IRDS scores were calculated using gene expression data from the GSE41814 dataset of 90 human NSCLCs treated on the JBR.10 randomized clinical trial. Patients underwent curative surgical resection followed by randomization to undergo observation or receive adjuvant cisplatin-based chemotherapy. Kaplan-Meier curves for disease-specific survival (DSS) stratified by receipt of chemotherapy for TSP-IRDS Low (≤ 4 , $n=42$) (B) and High (>4 , $n=48$) (C) patients. *P*-values were determined using log-rank tests.

Supplemental Table S1. Clonogenic survival of NSCLC cell lines after cytotoxic

therapy. Clonogenic survival fraction after treatment with cisplatin (0.5 µg/mL), etoposide (0.1 µg/mL), ionizing radiation (5 Gy) or SAR302503 (1000 nM). Values represent mean and standard error of mean (SEM). Data in column 2 denote tumor subgroups identified by K-means clustering of NSCLC cell lines by survival fraction.

Supplemental Table S2. Gene expression patterns correlating with SAR sensitivity.

Gene expression values were collected from the Cancer Cell Line Encyclopedia (CCLE) for cell lines in Supplemental Table S1. Genes with significant correlation or anti-correlation with clonogenic survival fraction were determined using Pearson correlation analysis (correlation threshold ± 0.6). Differentially expressed genes between SAR sensitive and SAR resistant cell lines (defined as survival fraction >0.2) were identified using Student's *t*-test (*P*-value threshold 0.05).